# Advanced X-ray Astrophysics Facility (AXAF): Calibration overview

S. L. O'Dell[a] and M. C. Weisskopf[b]

[a]NASA Marshall Space Flight Center, ES84
Huntsville, AL 35812 USA

[b]NASA Marshall Space Flight Center, ES01
Huntsville, AL 35812 USA

## ABSTRACT

The Advanced X-ray Astrophysics Facility (AXAF), the x-ray component of NASA's Great Observatories, will launch in 1999. As integration and testing of the flight system are concluding, analysis of the ground calibration data continues. This analysis verifies AXAF's unique capabilities for high-resolution imaging and for high-resolution dispersive spectroscopy. However, it finds unexpectedly high ($\approx 10\%$) residuals between the data and the model for effective area of the AXAF optics. Reconciling the physical model with the data, to an accuracy of a few percent, remains a goal of the analysis and interpretation of the calibration data.

**Keywords:** AXAF, space missions, x rays, calibration, grazing-incidence optics, gratings, detectors, x-ray imaging, x-ray spectroscopy.

## 1. INTRODUCTION

The Advanced X-ray Astrophysics Facility (AXAF) will join the Hubble Space Telescope (HST) and the Compton Gamma-Ray Observatory (CGRO) as one of NASA's "Great Observatories". AXAF provides unprecedented capabilities for sub-arcsecond imaging and spectrometric imaging and for high-resolution dispersive spectroscopy, over the x-ray band 0.08–10 keV (wavelength range 15–0.12 nm). With these capabilities, scientists will probe a wide variety of high-energy phenomena in a broad range of astronomical objects.

AXAF is a NASA-provided user facility, which will serve the international astronomical community for the next decade. It is the product of the efforts of several commercial, academic, and government organizations. NASA Marshall Space Flight Center (MSFC, Huntsville, Alabama) manages the Project; TRW Space and Electronics Group (Redondo Beach, California) serves as the prime contractor; and the Smithsonian Astrophysical Observatory (SAO, Cambridge, Massachusetts) is responsible for ground operations.

Invited paper, in *X-Ray Optics, Instruments, and Missions*, R. B. Hoover and A. B. Walker, eds., *Proc. SPIE* **3444**, 1998.
S.L.O.: odell@cosmos.msfc.nasa.gov; 256-544-7708.
M.C.W.: martin@cosmos.msfc.nasa.gov; 256-544-7740.

**Figure 1.** Photograph of the AXAF flight system (less solar panels) upon removal from the thermal-vacuum chamber at TRW. Photograph is from TRW.

In 1978, NASA conducted the phase-A study leading to the definition of the AXAF mission. During the intervening 20 years, several significant milestones transpired, leading to the planned launch in 1999:

**1985** Completion of the Phase-B study with x-ray testing of the Technology Mirror Assembly at MSFC.

**1988** Approval of the program as a new start and selection of TRW as prime contractor.

**1991** Selection of SAO for the science center and x-ray testing of the (uncoated) largest mirrors at MSFC.

**1992** Restructuring of the AXAF mission.

**1996** Completion of the mirror assembly at Kodak.

**1997** X-ray calibration of the observatory at MSFC.

**1998** Assembly and thermal-vacuum testing (Figure 1) of the flight system at TRW.

We begin by describing AXAF's mission (§2) to serve as NASA's premier facility for x-ray astrophysics. Then we briefly discuss the AXAF systems (§3) and the AXAF ground calibration (§4), both of which we have described in more detail in previous overviews.[1–3] Finally, we conclude (§5) with a review of unresolved issues in interpreting the results of the ground calibration.

## 2. AXAF'S MISSION

AXAF's mission is to serve the international science community. In this section, we summarize AXAF's key performance capabilities (§2.1), science objectives (§2.2), and mission parameters (§2.3).

### 2.1. Science capabilities

AXAF will be a unique x-ray-astronomy facility for high-resolution imaging (§2.1.1) and for high-resolution spectroscopy (§2.1.2). Indeed, AXAF's performance advantage over other x-ray observatories is analogous to that of the Hubble Space Telescope (HST) over ground-based observatories.

#### 2.1.1. Imaging performance

The angular resolution of AXAF is be about an order of magnitude better than any previous or planned x-ray observatory. Figures 2 and 3 illustrate AXAF's capability for sub-arcsecond imaging, demonstrated during the ground calibration.[4,5]

AXAF's point spread function (PSF, Figure 2), as measured during ground calibration, has a full width at half maximum (FWHM) less than 0.5 arcsec and a half-power diameter (HPD) less than 1 arcsec. The prediction for on-orbit encircled-energy fraction (Figure 3) shows that, throughout the AXAF energy band, a 1-arcsec-diameter circle encloses at least half the flux from a point source. The weakness of the energy dependence (resulting from diffractive scattering by surface microroughness) attests to the excellent superpolished finish of the AXAF optics.

Owing to the presence of a CCD focal-plane imaging spectrometer, AXAF offers the unique capability for high-resolution imaging with moderately good spectral resolution (Figure 4). AXAF's CCD imaging detectors provide a spectral resolving power ($E/\Delta E$) of 10 to 50 for energies between 0.5 and 7 keV.

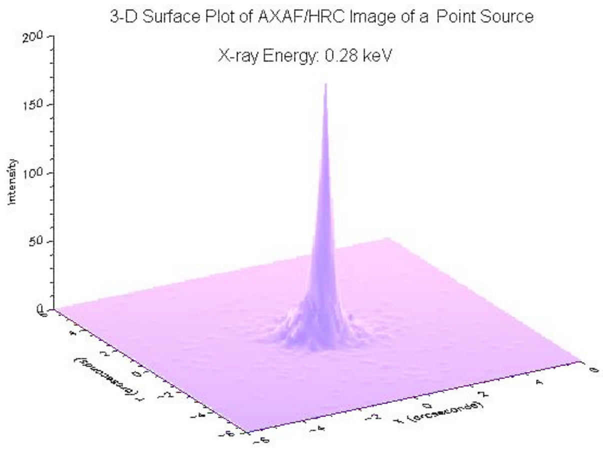


**Figure 2.** Point spread function (PSF) of the AXAF optics with the High-Resolution Camera (HRC), as measured during ground calibration of the AXAF observatory. The combined (optics and detector) full-width at half maximum is less than 0.5 arcsec. Surface plot is from the HRC team.

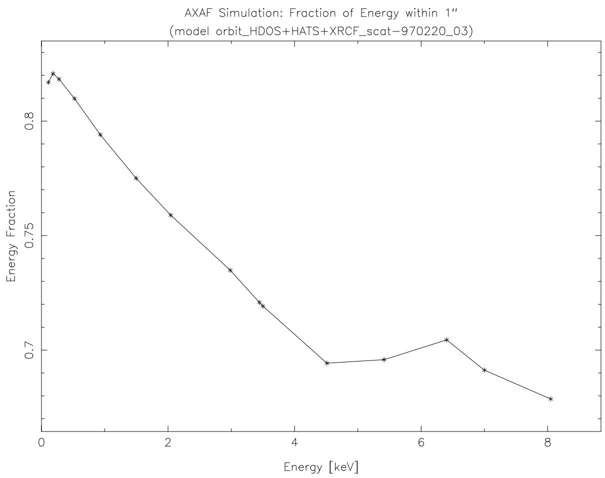


**Figure 3.** Predicted on-orbit encircled-energy fraction for the AXAF optics. Plot is from the AXAF Telescope Science and Mission Support Team (MST).

#### 2.1.2. Spectroscopic performance

The unprecedented angular resolution of the AXAF optics, combined with AXAF's micro-ruled objective transmission gratings (OTGs), provides the capability for high-resolution dispersive spectroscopy. AXAF provides two sets of OTGs — the Low-Energy Transmission Grating (LETG), optimized for the longer x-ray wavelengths, and the High-Energy Transmission Gratings (HETG), for the shorter wavelengths. Taking advantage of the different

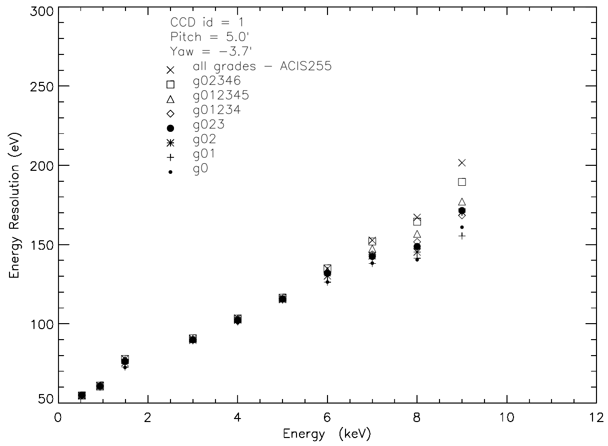


**Figure 4.** Energy resolution of the AXAF CCD Imaging Spectrometer (ACIS). The plot shows the measured energy resolution, for various grade selections, of the I1 (front-side) CCD on ACIS-I. Plot is from the ACIS team.

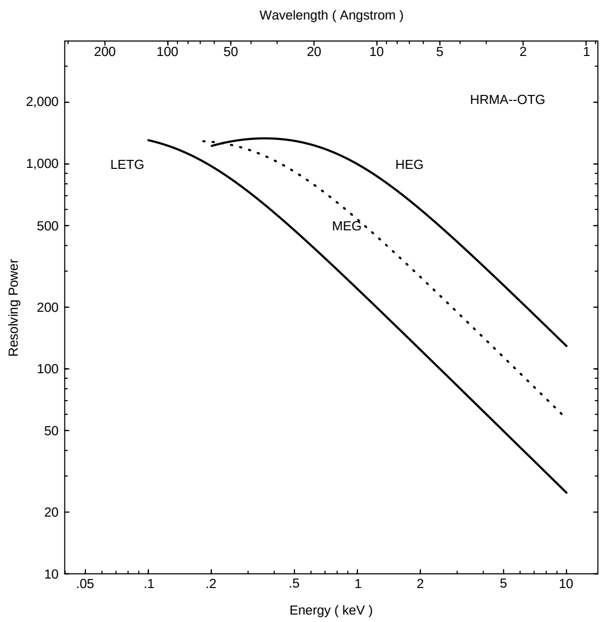


**Figure 5.** Specified spectral resolving power of AXAF OTGs. Preliminary results indicate slightly better performance. Plot is from the AXAF Project Science team.

energy response of AXAF's 4 mirror shells, the HETG employs 2 types of gratings, with slightly rotated dispersion directions, to give high spectral resolution over its entire energy range. Hence, with an appropriate combination of AXAF's three types of gratings, AXAF allows measurements with spectral resolving power (Figure 5) of $(\lambda/\Delta\lambda) = (E/\Delta E) > 500$ for wavelengths $\lambda > 0.4$ nm (energies $E < 3$ keV). Indeed, the ground calibration measured resolving powers approaching 2000 at the longest wavelengths in the AXAF spectral band (Figure 6).

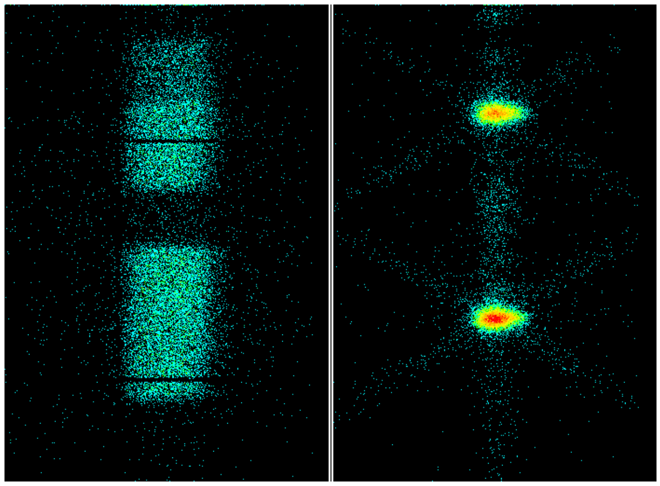

**Figure 6.** Line spread function (LSF) of the AXAF Low-Energy Transmission Grating Spectrometer (LETGS). The right image was obtained, during ground calibration, while dithering the detector; the left, a reconstructed (de-dithered) image, shows aluminum lines at 16.007 nm and 16.169 nm, at a resolving power of nearly 2000. (The image's elongation results from the 2-arcsec extent of the source.) Images are from the LETG team.

## 2.2. Science objectives

X rays result from highly energetic processes — thermal processes in plasmas with temperatures of millions of degrees or nonthermal processes, such as synchrotron emission or scattering from very hot or relativistic electrons. Consequently, x-ray sources are frequently exotic:

- Supernova explosions and remnants, where the explosion shocks the ambient interstellar medium or a pulsar (rotating neutron star) powers the emission.
- Accretion disks or jets around stellar-mass neutron stars or black holes.
- Accretion disks or jets around massive black holes in galactic nuclei.
- Hot gas in clusters of galaxies and in galaxies, which traces the gravitational field for determining mass.
- Hot gas in stellar coronas, especially during flares (coronal mass ejection).

Here we give a few examples of simulations which indicate the potential of AXAF for investigating these processes and astronomical objects through high-resolution (§2.2.1) imaging and high-resolution spectroscopy (§2.2.2).

### 2.2.1. Imaging objectives

AXAF's capability for high-resolution imaging (§2.1.1) enables detailed high-resolution studies of the structure of extended x-ray sources, including supernova remnants (Figure 7), astrophysical jets (Figure 8), and hot gas in galaxies and clusters of galaxies. The supplementary capability for spectrometric imaging allows studies of structure, not only in x-ray intensity, but in temperature and in chemical composition. Through these observations, astronomers will address several of the most exciting topics in contemporary astrophysics — *e.g.*, galaxy mergers, dark matter, and the cosmological distance scale.

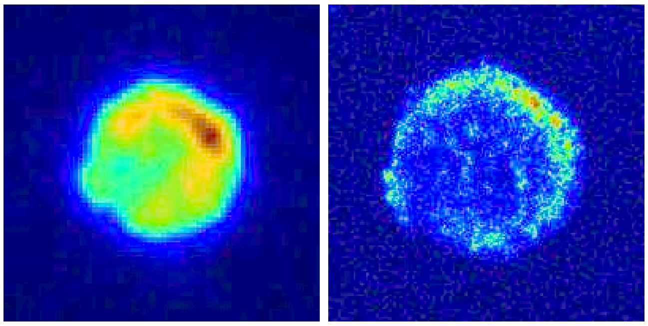

**Figure 7.** Comparison of an x-ray image (left) of the Tycho supernova remnant with one at 10-times-better angular resolution (right). AXAF's angular resolution is be about another factor-of-10 better than the best images obtained with any other x-ray observatory. Images are from the AXAF Science Center (ASC).

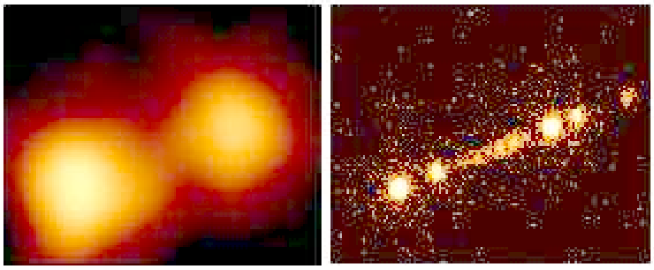

**Figure 8.** Comparison of an x-ray image (left) of the jet in the galaxy M87 with a simulated AXAF image (right). Images are from the AXAF Science Center (ASC).

In addition to mapping the structure of extended sources, the high angular resolution permits studies of ensembles of discrete sources, which would otherwise be impossible owing to source confusion. Thus, AXAF observations will isolate individual stars in clusters and star-forming regions and individual x-ray binaries in nearby normal galaxies. Furthermore, high-angular-resolution observations with AXAF's low-noise focal-plane detectors will obtain photon-limited, deep-field exposures which are likely to resolve most of the extragalactic cosmic x-ray background into faint, discrete sources.

### 2.2.2. Spectroscopic objectives

Owing to their unprecedented clarity, AXAF images will be visually striking and provide new insights into the nature of x-ray sources. Equally important to the imaging science (§2.2.1), will be AXAF's unique contributions to high-resolution dispersive spectroscopy. Indeed, as the capability for visible-light spectroscopy begat the field of astrophysics about a century ago, high-resolution x-ray spectroscopy will contribute profoundly to the understanding of the physical processes in cosmic x-ray sources.

High-resolution x-ray spectroscopy is the essential tool for diagnosing conditions in hot plasmas: It provides information for determining the temperature, density, elemental abundance, and ionization stage of x-ray-emitting plasma. The high spectral resolution of AXAF isolates individual lines from the myriad of spectral lines which would overlap at lower resolution Furthermore, it enables the determination of flow and turbulent velocities, through the measurement of Doppler shifts and widths.

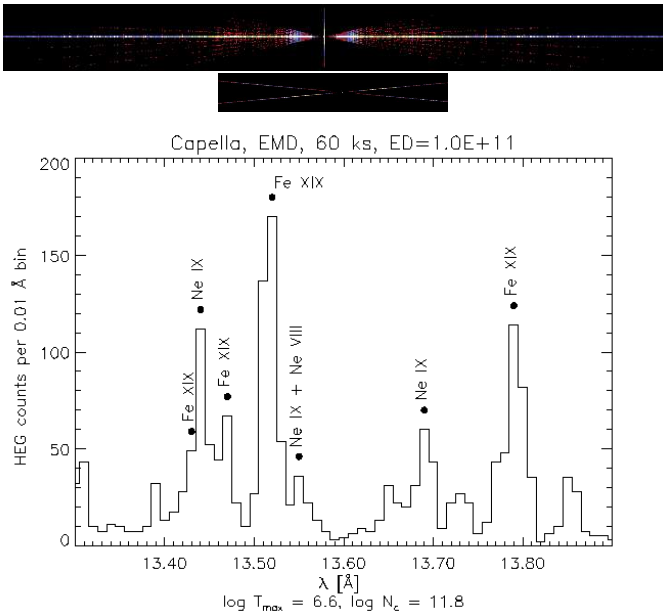


**Figure 9.** Simulation of the image of the spectrum of the stellar corona of Capella, as viewed with the LETGS (top) and HETGS (middle). The plot (bottom), over a small fraction of the full spectrum, illustrates the use of high-resolution spectroscopy to isolate individual lines for use as plasma diagnostics. Images and plot are from the Joint Institute for Laboratory Astrophysics (JILA).

Dispersive spectroscopy achieves its highest resolution for spatially unresolved sources. Thus, OTG observations will focus on stellar coronas (Figure 9), x-ray binaries, and active galactic nuclei. However, at somewhat lower spectral resolution, AXAF OTG observations are useful for studies of the more compact supernova remnants and cooling flows in clusters of galaxies (Figure 10), as well.

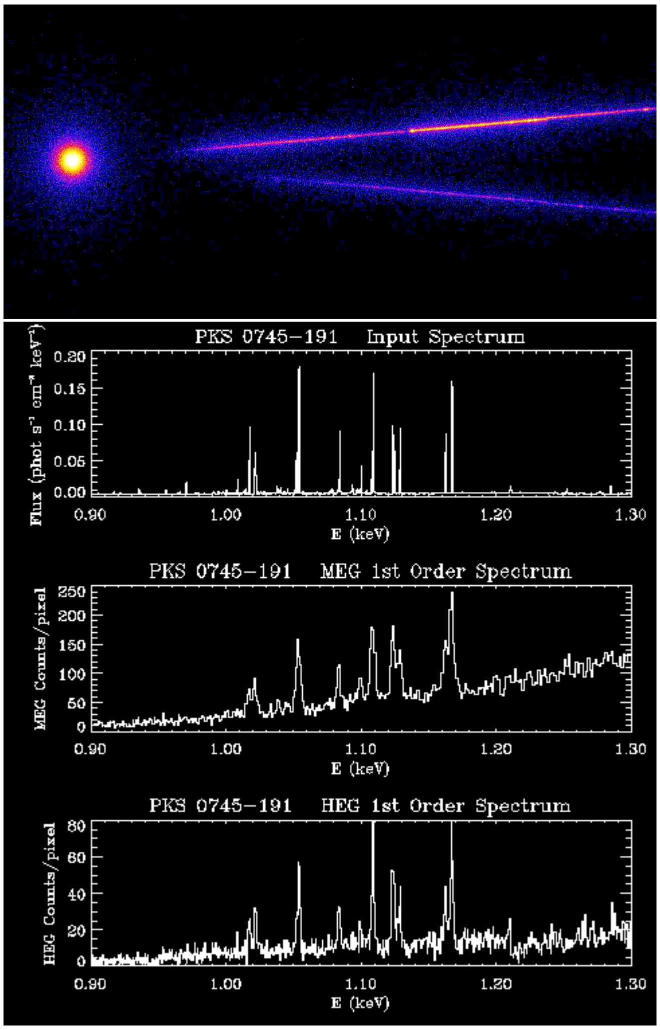


**Figure 10.** Simulation of the image of the HETGS spectrum of the cooling flow cluster PKS 0745-191. The image (top) shows the positive orders of the Medium-Energy Gratings (MEG) dispersed to the upper right and the High-Energy Gratings (HEG) dispersed to the lower right. The plots (bottom) show (from top to bottom) the model input spectrum, the MEG response, and the HEG response. Simulated image and plots are from the AXAF Science Center (ASC).

Besides observing the emission spectra of cosmic sources, AXAF high-resolution spectroscopy will also probe the interstellar medium through its absorption of x rays from bright sources. Such observations of absorption spectra provide information on both interstellar gas and dust — the latter through the analysis of extended x-ray absorption fine structure[6,7] (EXAFS) and x-ray absorption near-edge structure[7] (XANES).

### 2.3. Mission parameters

The space-shuttle *Columbia* will carry and deploy the AXAF into a low earth orbit, as NASA's Space Transportation System mission STS-93. After deployment from the *Columbia* orbiter at an altitude of about 240 km (150 nautical miles), the Inertial Upper Stage (IUS), a two-stage solid-fuel rocket booster developed by the Boeing Company Defense and Space Group (Seattle, Washington) for the US Air Force, will propel the AXAF flight system into a highly elliptical transfer orbit. Then AXAF's Internal Propulsion System (IPS), built by TRW, will place the flight system into its operational orbit — 140-Mm (87,000-nautical-mile) apogee and 10-Mm (6,200-nautical-mile) perigee, with a 28.5° initial inclination (Figure 11).

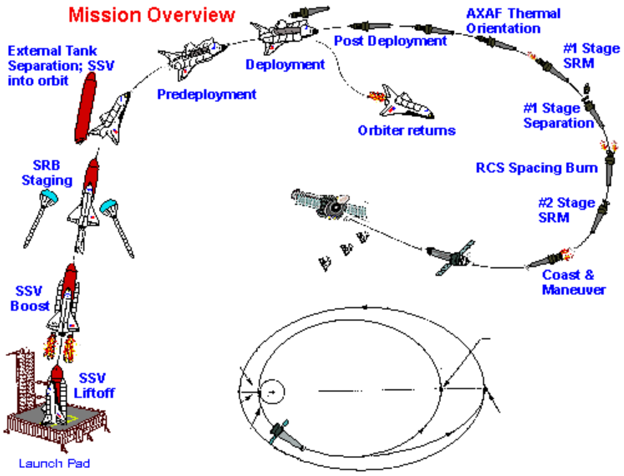


**Figure 11.** Depiction of AXAF's launch through insertion into its operational, highly elliptical orbit.

AXAF's highly elliptical orbit, with an orbital period of 2.7 days, results in a high efficiency for observing. The fraction of the sky occulted by the earth is small over most of the orbital period, as is the fraction of the time when detector backgrounds are high as the flight system dips into Earth's radiation belts. Consequently, more than 85% of the time is available for observing and uninterrupted observations lasting 2.3 days are possible.

The specified design life of the mission is 5 years; however, the design has sized all expendables (propulsion gas etc.) to allow operation for more than 10 years. Based upon the experience with previous major astronomical satellites and upon the response of the astronomy user community to AXAF's first NASA Research Announcement (NRA), AXAF's observing time is likely to be significantly oversubscribed for the next decade. Indeed, for AXAF's Cycle-1 proposal peer review, the requested observing time was 7 times that available!

# 3. AXAF SYSTEMS

## 3.1. Flight system

With the IUS attached, the AXAF will be the largest payload ever deployed by an STS space shuttle. Fully deployed, the AXAF flight system is 13.8-m (45.3-ft) long by 4.2-m (14-ft) diameter, with a 19.5-m (64-ft) solar-panel wingspan. With extensive use of graphite-composite structures, the mass of the AXAF flight system is 4,800 kg (weight of 10,600 pounds). The AXAF flight system (Figure 12) comprises 3 major modules or systems — the Telescope System (§3.1.1), the Integrated Science Instrument Module (§3.1.2), and the Spacecraft Module (§3.1.3). Here, we briefly describe these major modules: One of our previous overviews[1] furnishes more details.

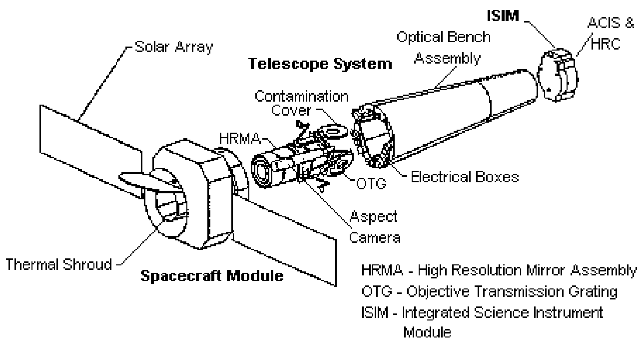


**Figure 12.** Expanded view of the AXAF flight system, showing several subsystems of the 3 major modules — the Telescope System, the Integrated Science Instrument Module, and the Spacecraft Module. Schematic drawing is from TRW.

### 3.1.1. Telescope system

The Eastman Kodak Company (Kodak, Rochester, New York) built the Telescope System. Its principal subsystems are the High-Resolution Mirror Assembly (HRMA, §3.2.1) and the Optical Bench Assembly (OBA). Composite Optics Incorporated (COI, San Diego, California) developed the critical light-weight composite materials for the OBA and for other AXAF structures. The Telescope System also provides mounts and mechanisms for the AXAF Observatory's 2 objective transmission gratings (§3.2.2). In addition to these major subsystems, Ball Aerospace and Technologies Corporation (Boulder, Colorado) fabricated the Aspect Camera Assembly,[8] a visible-light telescope and CCD camera which attaches to and is coupled with the Telescope System through a Fiducial-light Transfer System, which essentially maps the x-ray focal plane onto the sky.

### 3.1.2. Integrated Science Instrument Module

Ball Aerospace and Technologies Corporation (Boulder, Colorado) built the Science Instrument Module[9] (SIM), which includes mechanisms for focussing and translating AXAF's focal-plane science instruments (§3.2.3). The Integrated Science Instrument Module (ISIM) denotes the SIM with the 2 focal-plane science instruments integrated.

### 3.1.3. Spacecraft module

TRW Space and Electronics Group (Redondo Beach, California) built the Spacecraft Module. It comprises 7 major subsystems:

1. The Pointing Control and Aspect Determination (PCAD) subsystem performs on-board attitude determination, solar-array control, slewing, pointing and dithering control, and momentum management.
2. The Communication, Command, and Data Management (CCDM) subsystem performs communications, command storage and processing, data acquisition and storage, and computational support, timing reference, and switching of primary electrical power for other AXAF systems or subsystems.
3. The Electrical Power Subsystem (EPS) generates, regulates, stores, distributes, conditions, and controls the primary electrical power.
4. The Thermal Control Subsystem (TCS) furnishes passive thermal control (where possible), heaters, and thermostats.
5. The structures and mechanical subsystem encompasses the spacecraft structures, mechanical interfaces among spacecraft subsystems and with the telescope system and external structures.
6. The propulsion subsystem comprises the Integral Propulsion Subsystem (IPS) and the Momentum Unloading Propulsion Subsystem (MUPS).
7. The flight software implements algorithms for attitude determination and control, command and telemetry processing and storage, and thermal and electrical power monitoring and control.

### 3.2. Observatory system

The Observatory comprises AXAF's x-ray subsystems — the High-Resolution Mirror Assembly (HRMA, §3.2.1), objective transmission gratings (§3.2.2), and focal-plane science instruments (§3.2.3). Elsewhere,[1,3] we give a more detailed description.

#### 3.2.1. High-Resolution Mirror Assembly

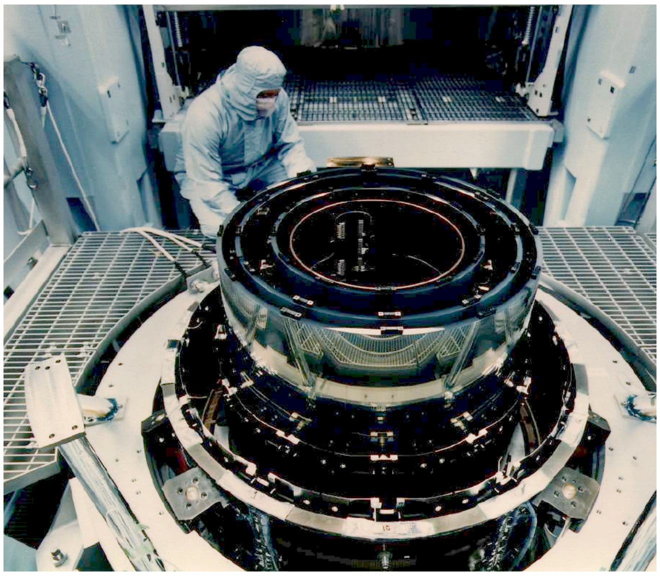

**Figure 13.** Photograph of the High-Resolution Mirror Assembly (HRMA) during alignment and assembly in the HRMA Alignment Tower at Kodak. In the picture, 7 of the 8 mirrors are already attached to the center aperture plate. Photograph is from Kodak.

Hughes Danbury Optical Systems (HDOS, Danbury, Connecticut) — now Raytheon Optical Systems Incorporated (ROSI) — precision figured and superpolished the 4-mirror-pair grazing-incidence x-ray optics out of Zerodur blanks from Schott Glaswerke (Mainz, Germany). Optical Coating Laboratory Incorporated (OCLI, Santa Rosa, California) then coated the optics with iridium, for optimal x-ray reflectance. The Eastman Kodak Company (Rochester, New York) aligned and assembled the mirrors into the 10-m-focal-length High-Resolution Mirror Assembly (HRMA, Figure 13), which includes thermal pre- and post-collimators and forward and aft contamination covers (Figure 14). The forward contamination cover houses 16 radioactive sources, developed by MSFC, for verifying transfer of the flux scale from the ground to orbit.[10,11] The precision figuring, superpolishing, alignment, and assembly of the HRMA enable AXAF to achieve its spectacular imaging performance (§2.1.1, Figure 2), already demonstrated during the ground calibration.[4,5]

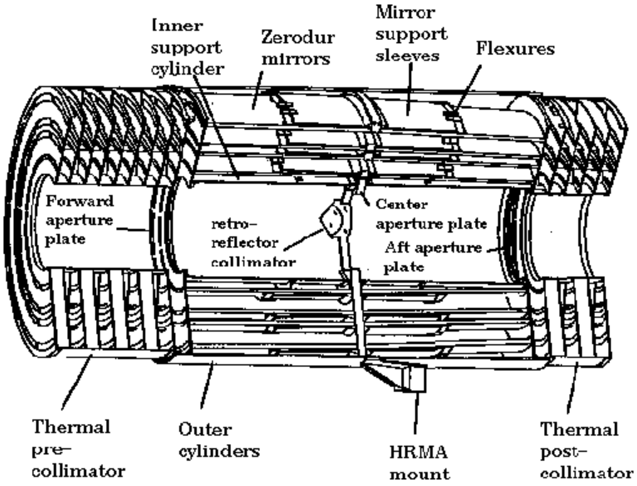


**Figure 14.** Schematic of the High-Resolution Mirror Assembly (HRMA), showing the 4 grazing-incidence (Wolter-1) paraboloid–hyperboloid mirror pairs mounted on the center aperture plate, and thermal pre- and post-collimators.

#### 3.2.2. Objective transmission gratings

Aft of the HRMA are 2 objective transmission gratings (OTGs) — the Low-Energy Transmission Grating (LETG) and the High-Energy Transmission Grating (HETG). Positioning mechanisms may insert either OTG into the converging beam, to disperse the x radiation onto the focal plane, producing high-resolution spectra read-out by one of the focal-plane detectors (§3.2.3).

**Low-Energy Transmission Grating (LETG)** The Space Research Institute of the Netherlands (SRON, Utrecht, Netherlands) and the Max-Planck-Institut für extraterrestrische Physik (MPE, Garching, Germany) designed and fabricated the Low-Energy Transmission Grating (LETG, Figure 15). The 540 grating facets, mounted 3 per module, lie tangent to the Rowland toroid which includes the focal plane. With free-standing gold bars of about 991-nm period, the LETG provides high-resolution spectroscopy from 0.08 to 2 keV (15 to 0.6 nm).

**High-Energy Transmission Grating (HETG)** The Massachusetts Institute of Technology (MIT, Cambridge, Massachusetts) designed and fabricated the High-Energy Transmission Grating (HETG, Figure 16). The HETG employs 2 types of grating facets — the Medium-Energy Gratings (MEG), mounted behind the HRMA's 2 outermost shells, and the High-Energy Gratings (HEG), mounted behind the HRMA's 2 innermost shells — oriented at slightly different dispersion directions. With

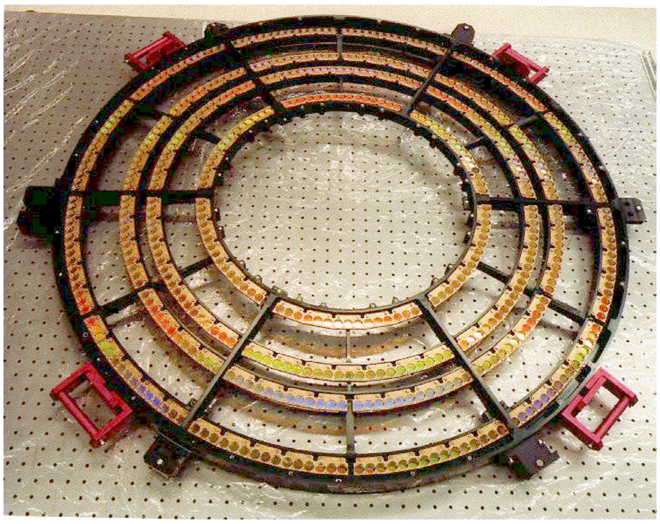

**Figure 15.** Photograph of the Low-Energy Transmission Grating (LETG). Photograph is from the LETG team.

polyimide-supported gold bars of 400-nm and 200-nm periods, respectively, the HETG provides high-resolution spectroscopy from 0.4 to 4 keV (MEG, 3 to 0.3 nm) and from 0.8 to 8 keV (HEG, 1.5 to 0.15 nm).

**Figure 16.** Photograph of the High-Energy Transmission Grating (HETG). Photograph is from the HETG team.

#### 3.2.3. Focal-plane science instruments

The Integrated Science Instrument Module (ISIM, §3.1.2) houses AXAF's 2 focal-plane science instruments — the (microchannel-plate) High-Resolution Camera (HRC) and the AXAF CCD Imaging Spectrometer (ACIS). Each instrument provides both an imaging detector (I) and a spectroscopy read-out detector (S) for reading out the high-resolution spectra dispersed by either of the AXAF Observatory's insertable OTGs.

**High-Resolution Camera (HRC)** The Smithsonian Astrophysical Observatory (SAO, Cambridge, Massachusetts) designed and fabricated the High-Resolution Camera[12] (HRC, Figure 17). Made of a single large-format (10-cm-square) microchannel plate, the HRC-I provides high-resolution imaging over a large (31-arcmin-square) field of view. Comprising 3 rectangular segments (3-cm-by-10-cm each) mounted end-to-end along the OTG dispersion direction, the HRC-S serves as the primary read-out detector for the LETG. Both detectors are coated with a cesium–iodide photocathode and covered with aluminized-polyimide UV/ion shields.

**Figure 17.** Photograph of the focal plane of the AXAF flight High-Resolution Camera (HRC). The HRC-I (imager) is at the bottom; the HRC-S (spectroscopic readout), the top. Photograph is from the HRC team.

**AXAF CCD Imaging Spectrometer (ACIS)** The Pennsylvania State University (PSU, University Park, Pennsylvania) and the Massachusetts Institute of Technology (MIT, Cambridge, Massachusetts) designed and fabricated the ACIS (Figure 18), with charge-coupled devices (CCDs) produced by MIT Lincoln Laboratory (Lexington, Massachusetts) and some subsystems and systems integration provided by Lockheed–Martin Astronautics (Littleton, Colorado). Comprising a 2-by-2 array of large-format (2.5-cm-square) CCDs, the ACIS-I provides high-resolution spectrometric imaging over a 17-arcmin-square field of view. The ACIS-S, a 6-by-1 array of the large-format CCDs mounted along the OTG dispersion direction, serves as the primary read-out detector for the HETG. Two of the AXAF-S CCDs are back-illuminated, to enhance the low-energy response. Both detectors are covered with aluminized-polyimide optical blocking filters.

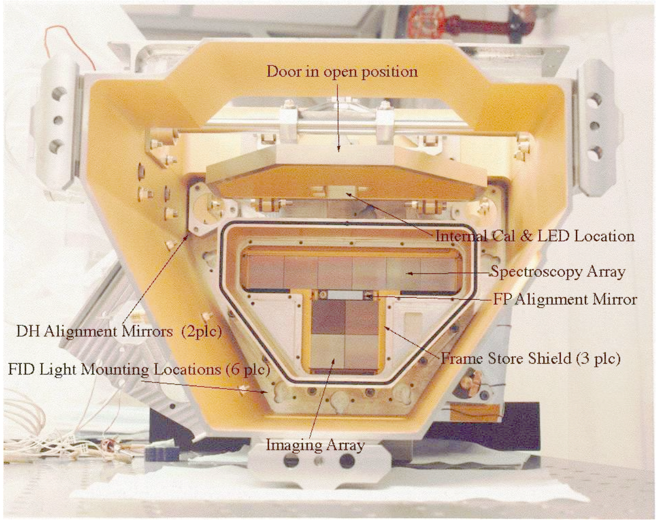


**Figure 18.** Photograph of the focal plane of the flight AXAF CCD Imaging Spectrometer (ACIS), prior to installation of the optical blocking filters. The ACIS-I (imager) is at the bottom; the ACIS-S (spectroscopic readout), the top. Photograph is from the ACIS team.

### 3.3. Ground system

The AXAF ground system comprises the Deep-Space Network (DSN, §3.3.1), the AXAF Operations Control Center (OCC, §3.3.2), and the AXAF Science Center (ASC, §3.3.3). In effect, the ground system is the 2-way path over which the astronomical community interacts with the AXAF to obtain science data.

#### 3.3.1. Deep-Space Network (DSN)

The Jet Propulsion Laboratory (JPL, managed for NASA by the California Institute of Technology, Pasadena, California) operates NASA's Deep-Space Network (DSN). Through its 3 antenna stations (Goldstone, California; Madrid, Spain; and Canberra, Australia), the DSN communicates directly with the AXAF spacecraft, up-linking commands and down-linking telemetered science and engineering data. During normal operations, DSN will contact, at 8-hour intervals, the AXAF spacecraft, which stores 16.8 hours (1.8 Gb) of data in its solid-state recorder.

#### 3.3.2. Operations Control Center (OCC)

Although originally conceived as a separate entity, the AXAF Operations Control Center (OCC) is now located in Cambridge, Massachusetts, and operated as part of the AXAF Science Center (ASC, §3.3.3). The AXAF prime contractor, TRW, staffs the OCC's Flight Operations Team (FOT), which is responsible for the control, health, and safety of the spacecraft. The OCC receives Observation Requests, which it uses to build the long-term schedule, Detailed Operations Timeline, and command loads to be sent to the spacecraft through the DSN. From the spacecraft, through the DSN, the OCC receives the telemetered data, converts its format, extracts the engineering stream, and analyses the engineering data. The OCC utilizes on-line software developed by MSFC and off-line software developed by the Computer Sciences Corporation (CSC, El Segundo, California).

#### 3.3.3. AXAF Science Center (ASC)

The Smithsonian Astrophysical Observatory (SAO), with the Massachusetts Institute of Technology (MIT), operates the AXAF Science Center (ASC). As AXAF's day-to-day interface with the scientific community, the ASC solicits observing proposals, provides proposal-preparation information and tools, organizes peer reviews on behalf of NASA, builds Observation Requests (OR) based on results of the peer review and calibration needs, and submits the OR to the OCC for scheduling. The ASC receives the re-formatted telemetry from the OCC, extracts the science stream, processes the science data, constructs time-tagged event lists for each observation, performs higher level data processing (*e.g.*, generates images and spectra), operates the data archive, maintains the calibration, and provides data, analysis tools, and other support to the user. The ASC is also responsible for developing and maintaining the software to support these functions.

## 4. GROUND CALIBRATION

The ground calibration of AXAF included an intensive and extensive calibration program for calibrating the full Observatory (§4.1) and its individual subsystems (§4.2). The calibration results (§4.3) clearly demonstrate that the AXAF Observatory provides the science capabilities (§2.1) — high-resolution (sub-arcsec) imaging and spectrometric imaging and high-resolution dispersive spectroscopy — to address its science objectives (§2.2). However, with a goal of a high accurate calibration, the calibration program is a tremendous effort which requires continued analysis and interpretation. Our previous overview[3] provides more details on the calibration.

## 4.1. Observatory calibration

From 1996 December until 1997 May, the AXAF teams calibrated the AXAF Observatory at the MSFC X-Ray Calibration Facility (XRCF, Figure 19). This followed a pre-calibration rehearsal at the XRCF, during the summer of 1996. The following organizations (in alphabetical order) contributed to this calibration:

- AXAF Science Center (ASC)
- Ball Aerospace & Technologies Corporation
- Eastman Kodak Company
- MIT & PSU ACIS team
- MIT HETG team
- MPE & SRON LETG team
- MSFC Project Science (PS)
- MSFC Systems Analysis & Integration Laboratory
- SAO HRC team
- SAO Mission Support Team (MST)
- SAO Telescope Science (TS)
- TRW Space & Electronics Group

**Figure 19.** Aerial photograph of the X-Ray Calibration Facility (XRCF) at NASA Marshall Space Flight Center (MSFC). The small building to the far left houses the X-ray Source System (XSS); the large building to the near right houses the instrument chamber, control room, and data processing. Photograph is from MSFC.

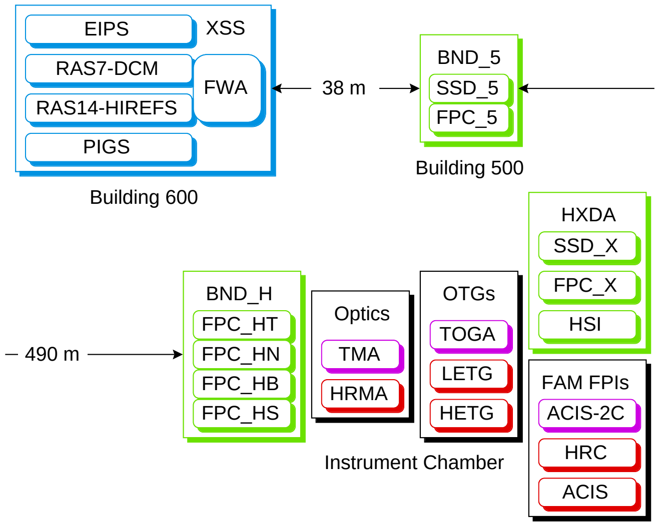


**Figure 20.** Schematic of x-ray sources and detectors during calibration of the AXAF Observatory at the XRCF and the pre-calibration rehearsal. Schematic is from the Project Science team.

The calibration of the AXAF Observatory and a pre-calibration rehearsal employed an extensive x-ray system (Figure 20). Providing a versatile range of x-ray parameters, the X-ray Source System[13] (XSS) comprises the Electron Impact Point Source (EIPS, from MSFC), 2 monochromators[14] — the Double Crystal Monochromator (DCM, from the National Institute of Standards and Technology) and the (reflection-grating monochromator) HIgh-Resolution Erect-Field Spectrometer (HIREFS$^{\mathrm{TM}}$, from Hettrick Scientific) — each with a with a Rotating Anode Source (RAS, from Rigaku), the Penning Ionization Gas-discharge Source (PIGS, from SAO), and a Filter-Wheel Assembly (FWA, from MSFC).

The XRCF incorporates 6 Beam-Normalization Detectors (BNDs) — 2 located approximately 38 m from the XSS and 4 approximately 520 m away, at the optics's entrance aperture in the XRCF instrument chamber (Figure 21). Except for one Solid-State Detector (SSD) close to the XSS, the BNDs are Flow Proportional Counters (FPCs). The SAO Mission Support Team provided the BNDs and the (focal-plane) HRMA X-ray Detector Assembly (HXDA), which together comprise the HRMA X-ray Detection System (HXDS).

Calibration of the Observatory used, of course, the flight High-Resolution Mirror Assembly (HRMA, §3.2.1) and flight objective transmission gratings (OTGs, §3.2.2) — the Low-Energy Transmission Grating (LETG) and the High-Energy Transmission Grating (HETG). The Eastman Kodak Company provided actuators and mechanisms for orienting the HRMA, for operating the forward

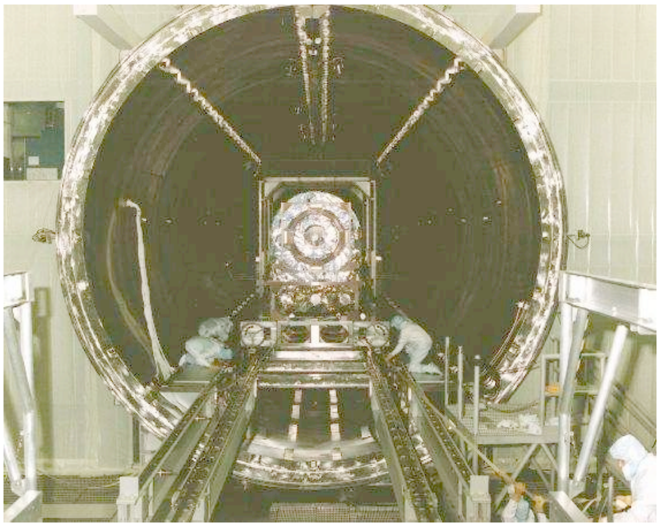

**Figure 21.** Photograph of the HRMA in the XRCF Instrument Chamber at MSFC. Photograph is from MSFC.

and aft contamination covers, for inserting the OTGs), and for functioning the 16 quadrant shutters used to isolate individual shell quadrants, which were especially useful for focussing.

For the pre-calibration rehearsal, the optic employed was the Technology Mirror Assembly (TMA), which was built and x-ray tested about a decade earlier to demonstrate the viability of technologies to be used for figuring and polishing optics for AXAF. Because the flight OTGs (LETG and HETG) are matched to the HRMA's geometry, the MIT HETG team custom built the TMA Objective Grating Assembly (TOGA), using flight-type gratings from the LETG and the HETG, to allow a realistic rehearsal of high-resolution-spectroscopy data collection and analysis.

Besides the flight focal-plane instruments (§3.2.3) — the High-Resolution Camera (HRC) and AXAF CCD Imaging Spectrometer (ACIS) — the calibration employed 4 non-flight detectors. The HRMA X-ray Detector Assembly (HXDA), designed and fabricated by SAO, comprises a Solid-State Detector (SSD) with aperture wheel, a Flow Proportional Counter (FPC) with aperture plate, and a microchannel-plate High-Speed Imager (HSI). In addition, the ACIS Two-Chip (ACIS-2C), custom built by MIT and SAO, served as an ACIS surrogate during rehearsal and calibration prior to arrival of the flight ACIS. To position the ACIS-2C flight detectors (HRC and ACIS) during the calibration of the Observatory, Ball Aerospace and Technologies Corporation built a Five-Axis Mount (FAM) as a surrogate for the flight Science Instrument Module (SIM, §3.1.2).

## 4.2. Subsystem calibrations

In addition to the joint system-level calibration of the AXAF Observatory at the XRCF, individual teams conducted extensive sub-system calibrations. The SAO Mission Support Team (MST) and the Physikalisch–Technische Bundesanstalt (PTB) is calibrating SSDs[15] and FPCs[16] from the HRMA X-ray Detector System, at the Berliner Elektronenspeicherring-Gesellschaft für Synchrotronstrahlung (BESSY). Using the precisely calculable synchrotron radiation from a countable number of electrons of known energy, absolute calibrations are, in principle, possible.

Furthermore, the SAO Mission Support Team (MST), with the Los Alamos National Laboratory (LANL) and Lawrence Berkeley National Laboratory (LBNL), is using the National Synchrotron Light Source (NSLS) at Brookhaven National Laboratory (BNL) and the Advanced Light Source[17] (ALS) at LBNL to determine[18–21] the optical constants of iridium coatings deposited on witness flats during qualification runs and coating of the AXAF optics. The objective is to combine these measurements of reflectance with the SAO-developed finite-element and ray-trace models to simulate the performance[4,5,22] of the HRMA.

Each of the OTG teams has used its own laboratories, BESSY, and other facilities for sub-system calibrations. The LETG team calibrated the LETG grating period and period variations at the Max-Planck-Institut für extraterrestrische Physik (MPE) and the transmission efficiency of individual gratings at BESSY. The HETG team calibrated[23,24] the HETG grating periods and period variations at MIT and the transmission efficiency[25,26] of individual ratings at MIT, NSLS, and BESSY.

Likewise, each of the focal-plane-instrument teams has performed sub-system calibrations at various locations. The SAO HRC team and the University of Leicester (UK) characterized and calibrated[27] microchannel plates MCPs[28,29] in their laboratories and measured atomic-edge structure of flight-like CsI-coated MCPs at the Daresbury Synchrotron Radiation Source (UK). With the Istituto e Osservatorio Astronomico G. S. Vaiana (Italy), SAO also characterized the UV/ion shields.[30,31] The ACIS team calibrated[32] CCD absolute efficiency using atomic-fluorescence sources at MIT[33] and synchrotron measurements at BESSY; they calibrated the energy scale and spectral resolution using a reflection- grating spectrometer at MIT.[34] In addition, they characterized the optical blocking filters at PSU[35] and, with SAO, at the NSLS.[36]

## 4.3. Summary of results

The AXAF science teams provide detailed results of the ground calibration in the Calibration Report, accessible through the Project Science calibration web page at `http://wwwastro.msfc.nasa.gov/xray/xraycal`. Release 1 of the Calibration Report occurred in 1997 October; release 2 is nearing completion. In addition to the Calibration Report, many of the initial results have appeared in these[37–41] and previous[4,5,12,28,29,42–47] proceedings. Here we recapitulate basic results for the key performance metrics of imaging resolution (§4.3.1) and of spectral resolution (§4.3.2). Then we address the more problematic topic of reconciling through-put (effective-area and efficiency) measurements with model predictions to the desired accuracy (§4.3.3).

### 4.3.1. Imaging resolution

The calibration results confirm AXAF's unprecedented capabilities for high-resolution imaging and spectrometric imaging.[4,5] As described earlier (§2.1.1), the calibration results (*e.g.*, Figure 2), show that the Observatory's on-axis full-width at half maximum (FWHM) and half-power diameter (HPD) are each less than an arcsecond. Consistent with these results, the performance prediction for the on-orbit encircled energy (*e.g.*, Figure 3) gives at least 50% of the flux included within a 1-arcsec circle for an on-axis source, over the entire AXAF energy band (0.08–10 keV).

Furthermore, the ACIS spectral resolution is excellent and fairly consistent with models for the CCD performance (Figure 4), at least for the front-illuminated CCDs.[39] As anticipated, the 2 back-illuminated CCDs in the ACIS-S array exhibit poorer energy resolution and are not yet modeled as accurately; however, their energy resolution is more than adequate for separation of OTG spectral orders.

### 4.3.2. Spectral resolution

The calibration results confirm AXAF's unprecedented capabilities for high-resolution dispersive spectroscopy. As described earlier (§2.1.2), the preliminary calibration results[44,46] (*e.g.*, Figure 6) are slightly better than the specified spectral resolving power (Figure 5). Thus, with selection of the appropriate OTG (LETG or HETG), AXAF provides spectral resolving power exceeding 500 up to a few keV.

### 4.3.3. Throughput

The philosophy guiding the calibration of AXAF is to employ system and sub-system calibration data to constrain theoretical and semi-empirical models for the performance of the individual sub-systems. In principle, the enormous ensemble of calibration data overdetermines model parameters and thus tightly constrains these models: "The model is the calibration." As yet, we have not attained this objective for models of throughput (effective area, efficiency, *etc.*, to the level of accuracy we desire and expect. Here, we highlight the current status of modeling the calibration measurements for HRMA effective area, OTG efficiency, and ACIS pile-up.

**HRMA effective area** The efforts to model the measured effective area of the HRMA to a few-percent accuracy have proved problematic.[4,37,42,43] While efforts continue with some success to identify and remove systematic differences among the efficiencies of the detectors, the measured effective area remains about 10% below model predictions, for energies above 2 keV (Figure 22).

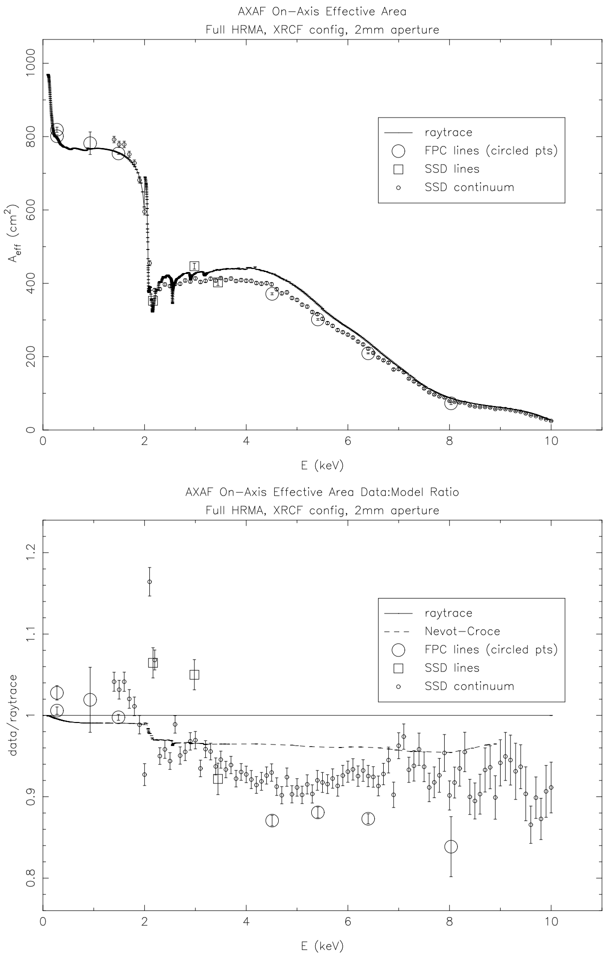


**Figure 22.** Comparison of model HRMA effective area with various data obtained during the Observatory calibration at the XRCF. Plots are from the Telescope Science and the Mission Support Team.

Currently, we believe that this discrepancy results, in part, because of different approaches used in modeling the effects of surface roughness. Basically, the synchrotron program to determine the optical constants of iridium-coated flats uses one technique, while the analysis of the Observatory calibration uses another. Specifically, the synchrotron program employs the Nevot–Croce approximation.[19,48,49] to calculate extinction of the specular radiation due to surface roughness, without regard to the angular distribution of the scattered radiation. In contrast, the HRMA ray-trace modeling explicitly calculates the angular distribution of the scattered radiation using scalar scattering theory.[50] Although these two approaches are, in principle, mutually consistent, their application may not be totally consistent and complete.[51]

In addition, other factors may affect the reflectance of the AXAF HRMA mirrors. For example, either gradients in the density of the iridium coating near its surface or the presence of molecular contamination on the coating's surface can alter the reflectance. In most reasonable cases, the former effect would decrease the reflectance, while the latter would increase it.[52,53]

**HETG and LETG efficiencies** Modeling of the HETG and LETG efficiencies, sub-system measurements, and the Observatory calibration data now agree to within about 15%[40,45,47] (Figure 23). While this is approximately the accuracy goal for the OTG calibrations, the HETG and LETG teams continue to refine models for the efficiency individual grating facets — including, bar shape, as well as size and spacing — and then synthesizing the efficiency of an ensemble of hundreds of individual facets. Note that, because the efficiencies are obtained by comparing OTG-in to OTG-out measurements, the determined values are independent of the HRMA effective area and any uncertainties associated with it.

**ACIS pile-up** Owing to the 3.3-s frame time of the ACIS CCDs in full-frame mode and the highly concentrated image produced by the HRMA, observations of bright sources can result in multiple photons striking the same or adjacent pixels during a given frame — *i.e.*, pile-up. Pile-up effects both energy redistribution and count-rate nonlinearity (Figure 24, from a report by ASC/ B. R. McNamara, at `http://asc.harvard.edu/cal/CIP/cip.html`). This — compounded by the complexity of event-recognition algorithms, grade selection, and split events — makes pile-up a challenge to treat accurately.[54]

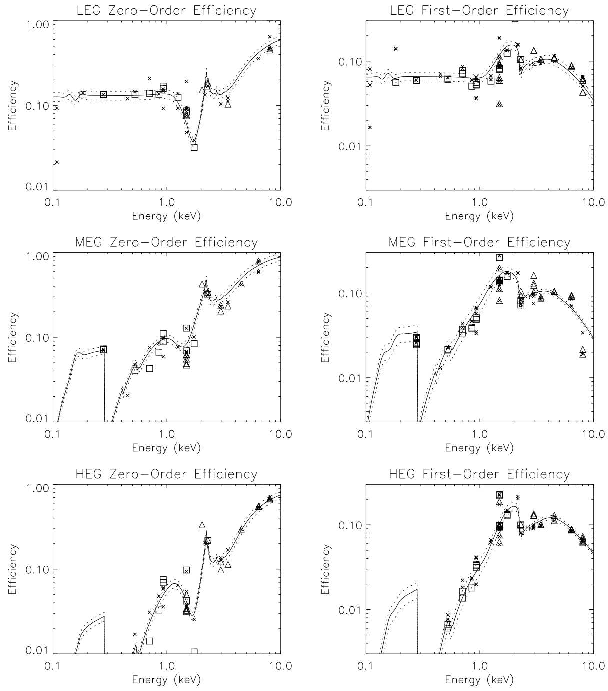


**Figure 23.** Comparison of modeled HETG and LETG efficiencies with various data obtained during the Observatory calibration at the XRCF. Plots are from the HETG team.

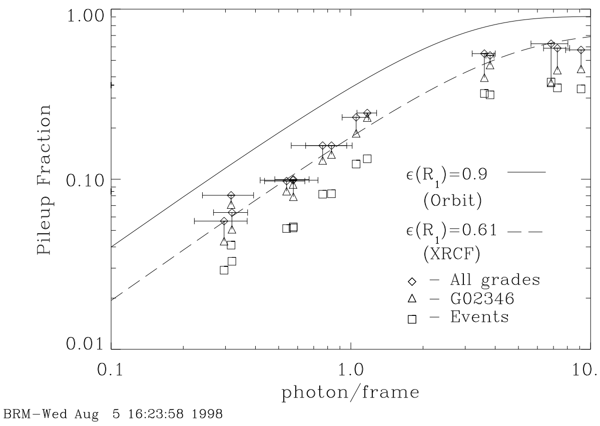


**Figure 24.** Comparison of model pile-up effects with data obtained during calibration of the AXAF Observatory at the XRCF. Plot is from the ASC.

## 5. CONCLUSION

The x-ray calibration of the AXAF Observatory (mirror assembly, transmission gratings, and focal-plane detectors) has verified the unique performance capabilities of AXAF for high-resolution (sub-arcsecond) imaging and spectrometric imaging and for high-resolution dispersive spectroscopy. Extensive and intensive analyses of the enormous database of system and sub-system calibration measurements continue, with the goal of calibrating the throughput of the Observatory, particularly its spectral dependence, to an accuracy of a few percent. Key to this is reconciling apparent discrepancies within the data sets and further developing the modeling of the data.

## 6. ACKNOWLEDGEMENTS

We recognize the efforts of the AXAF teams which have contributed to the calibration planning, data acquisition, data analysis and interpretation, and reporting. In preparing this overview, we have used figures drawn from their work.

## APPENDIX A. AXAF WEB SITES

The following lists several AXAF-related sites on the World-Wide Web (WWW). Most sites are cross-linked to one another.

`http://asc.harvard.edu/` AXAF Science Center (ASC), operated for NASA by the Smithsonian Astrophysical Observatory (SAO).

`http://wwwastro.msfc.nasa.gov/xray/axafps.html` AXAF Project Science, at the NASA Marshall Space Flight Center (MSFC).

`http://hea-www.harvard.edu/HRC/` AXAF High-Resolution Camera (HRC) team, at the Smithsonian Astrophysical Observatory (SAO).

`http://www.astro.psu.edu/xray/axaf/axaf.html` AXAF CCD Imaging Spectrometer (ACIS) team at the Pennsylvania State University (PSU).

`http://acis.mit.edu/` AXAF CCD Imaging Spectrometer (ACIS) team at the Massachusetts Institute of Technology (MIT).

`http://www.rosat.mpe-garching.mpg.de/axaf/` AXAF Low-Energy Transmission Grating (LETG) team at the Max-Planck Institut für extraterrestrische Physik (MPE).

`http://space.mit.edu/HETG/` AXAF High-Energy Transmission Grating (HETG) team, at the Massachusetts Institute of Technology (MIT).

`http://hea-www.harvard.edu/MST/` AXAF Mission Support Team (MST), at the Smithsonian Astrophysical Observatory (SAO).

`http://elses1.msfc.nasa.gov/xcfdoc/xAhome.html` X-Ray Calibration Facility (XRCF), at the NASA Marshall Space Flight Center (MSFC).

`http://snail.msfc.nasa.gov/sa/axaf/axaf.html` AXAF page of the Mission Operations Laboratory at the NASA Marshall Space Flight Center (MSFC).

`http://ipa.harvard.edu/` AXAF Operations Control Center, operated for NASA by the Smithsonian Astrophysical Observatory (SAO).

## REFERENCES

1. M. C. Weisskopf, S. L. O'Dell, R. F. Elsner, and L. P. Van Speybroeck, "Advanced X-ray Astrophysics Facility (AXAF): An overview," in *X-Ray and Extreme Ultraviolet Optics*, R. B. Hoover and A. B. Walker, eds., *Proc. SPIE* **2515**, pp. 312–329, 1995.
2. M. C. Weisskopf, S. L. O'Dell, and L. P. Van Speybroeck, "Advanced X-ray Astrophysics Facility (AXAF): An overview," in *Multilayer and Grazing Incidence X-Ray/EUV Optics III*, R. B. Hoover and A. B. Walker, eds., *Proc. SPIE* **2805**, pp. 2–7, 1996.
3. M. C. Weisskopf and S. L. O'Dell, "Calibration of the AXAF observatory: Overview," in *Grazing Incidence and Multilayer X-Ray Optical Systems*, R. B. Hoover and A. B. Walker, eds., *Proc. SPIE* **3113**, pp. 2–17, 1997.
4. L. P. Van Speybroeck, D. Jerius, R. Edgar, T. Gaetz, P. Zhao, and P. Reid, "Performance expectation versus reality," in *Grazing Incidence and Multilayer X-Ray Optical Systems*, R. B. Hoover and A. B. Walker, eds., *Proc. SPIE* **3113**, pp. 89–104, 1997.
5. T. J. Gaetz, R. J. Edgar, M. D. Freeman, W. A. Podgorski, L. P. Van Speybroeck, P. Zhao, J. Kolodziejczak, and M. Weisskopf, "Focus and alignment of the AXAF optics," in *Grazing Incidence and Multilayer X-Ray Optical Systems*, R. B. Hoover and A. B. Walker, eds., *Proc. SPIE* **3113**, pp. 77–88, 1997.
6. A. Evans, "Exafs studies of interstellar dust," *Mon. Not. Roy. Astron. Soc.* **223**, pp. 219–224, 1986.
7. J. W. Woo, "EXAFS and XANES: New astrophysical tools to study the solid-state structure of interstellar grains," *Astrophys. J. Lett.* **447**, pp. 129–132, 1995.
8. D. L. Michaels, "Performance of the aspect camera assembly for the Advanced X-Ray Astrophysics Facility," in *Acquisition, Tracking, and Pointing XII*, M. K. Masten and L. A. Stockum, eds., *Proc. SPIE* **3365,**, pp. 232–241, 1998.
9. M. A. Skinner and S. P. Jordan, "AXAF: The Science Instrument Module," in *EUV, X-Ray, and Gamma-Ray Instrumentation for Astronomy VIII*, O. H. Siegmund and M. A. Gummin, eds., *Proc. SPIE* **3114**, pp. 2–10, 1997.
10. R. F. Elsner, M. K. Joy, S. L. O'Dell, B. D. Ramsey, and M. C. Weisskopf, "Ground-to-orbit transfer of the AXAF-I flux scale: In-situ contamination monitoring of x-ray telescopes," in *Multilayer and grazing incidence X-ray/EUV optics for astronomy and projection lithography*, R. B. Hoover and A. B. Walker, eds., *Proc. SPIE* **2279**, pp. 332–342, 1994.

11. R. F. Elsner, S. L. O'Dell, B. D. Ramsey, A. F. Tennant, M. C. Weisskopf, J. J. Kolodziejczak, D. A. Swartz, D. E. Engelhaupt, G. P. Garmire, J. A. Nousek, M. W. Bautz, T. J. Gaetz, and P. Zhao, "Calibration results for the AXAF flight contamination monitor," in *X-Ray Optics, Instruments, and Missions*, R. B. Hoover and A. B. Walker, eds., *Proc. SPIE* **3444**, these proceedings, 1998.

12. S. S.Murray, J. H. Chappell, A. T. Kenter, K. Kobayashi, R. P. Kraft, G. R. Meehan, M. V. Zombeck, G. W. Fraser, J. F. Pearson, J. E. Lees, A. N. Brunton, S. E. Pearce, M. Barbera, A. Collura, and S. Serio, "AXAF High-Resolution Camera (HRC)," in *EUV, X-Ray, and Gamma-Ray Instrumentation for Astronomy VIII*, O. H. Siegmund and M. A. Gummin, eds., *Proc. SPIE* **3114**, pp. 11–25, 1997.

13. J. J. Kolodziejczak, R. A. Austin, R. F. Elsner, M. K. Joy, M. E. Sulkanen, E. M. Kellogg, and B. J. Wargelin, "X-ray source system at the Marshall Space Flight Center X-Ray Calibration Facility," in *X-Ray and Extreme Ultraviolet Optics*, R. B. Hoover and A. B. Walker, eds., *Proc. SPIE* **2515**, pp. 420–435, 1995.

14. D. A. Swartz, R. F. Elsner, J. J. Kolodziejczak, S. L. O'Dell, A. F. Tennant, M. E. Sulkanen, M. C. Weisskopf, and R. J. Edgar, "On the use of monochromators during AXAF calibration," in *X-Ray Optics, Instruments, and Missions*, R. B. Hoover and A. B. Walker, eds., *Proc. SPIE* **3444**, these proceedings, 1998.

15. S. Kraft, F. Scholze, R. Thornagel, G. Ulm, W. C. McDermott, and E. M. Kellogg, "High-accuracy calibration of the HXDS HPGe detector at the PTB radiometry laboratory at BESSY," in *EUV, X-Ray, and Gamma-Ray Instrumentation for Astronomy VIII*, O. H. Siegmund and M. A. Gummin, eds., *Proc. SPIE* **3114**, pp. 101–112, 1997.

16. J. M. Auerhammer, G. Brandt, F. Scholze, R. Thornagel, G. Ulm, W. C. McDermott, T. J. Norton, I. N. Evans, and E. M. Kellogg, "High-accuracy calibration of the HXDS flow proportional counter for AXAF at the PTB laboratory at BESSY," in *X-Ray Optics, Instruments, and Missions*, R. B. Hoover and A. B. Walker, eds., *Proc. SPIE* **3444**, these proceedings, 1998.

17. J. H. Underwood, E. M. Gullikson, M. Kroike, and P. J. Batson, "Beamline for metrology of x-ray/euv optics at the Advanced Light Source," in *Grazing Incidence and Multilayer X-Ray Optical Systems*, R. B. Hoover and A. B. Walker, eds., *Proc. SPIE* **3113**, pp. 214–221, 1997.

18. R. L. Blake, A. J. Burek, J. J. Fitch, D. E. Graessle, D. A. Schwartz, R. Soufli, E. M. Gullikson, A. Stonas, and J. H. Underwood, "Feasibility study of ALS beamline 6.3.2 in the calibration of AXAF: Initial reflectivity results," in *X-Ray Optics, Instruments, and Missions*, R. B. Hoover and A. B. Walker, eds., *Proc. SPIE* **3444**, these proceedings, 1998.

19. D. E. Graessle, A. J. Burek, J. J. Fitch, B. Harris, D. A. Schwartz, and R. L. Blake, "Optical constants from synchrotron reflectance measurements of AXAF witness mirrors 2–12 keV," in *Grazing Incidence and Multilayer X-Ray Optical Systems*, R. B. Hoover and A. B. Walker, eds., *Proc. SPIE* **3113**, pp. 52–64, 1997.

20. J. J. Fitch, R. L. Blake, A. J. Burek, A. M. Clark, D. E. Graessle, B. Harris, D. A. Schwartz, and J. Sweeney, "AXAF synchrotron witness mirror calibrations 2–12 keV," in *Grazing Incidence and Multilayer X-Ray Optical Systems*, R. B. Hoover and A. B. Walker, eds., *Proc. SPIE* **3113**, pp. 30–39, 1997.

21. D. E. Graessle, J. J. Fitch, B. Harris, P. Hsieh, D. Nguyen, J. Hughes, D. A. Schwartz, and R. L. Blake, "Calibration of AXAF mirrors using synchrotron radiation," *Bull. Am. Astron. Soc.* **187**, p. 7705, 1995.

22. D. Jerius, L. Cohen, R. Edgar, M. Freeman, T. Gaetz, J. Hughes, E. M. Kellogg, W. Podgorski, D. Schwartz, L. Van Speybroeck, and P. Zhao, "Predicted x-ray performance of the AXAF high-resolution mirror during ground calibration at the Marshall Space Flight Center," *Bull. Am. Astron. Soc.* **187**, p. 7706, 1995.

23. D. Dewey, D. N. Humphries, G. Y. McLean, and D. A. Moschella, "Laboratory calibration of x-ray transmission diffraction gratings," in *EUV, X-Ray, and Gamma-Ray Instrumentation for Astronomy V*, O. H. Siegmund and J. V. Vallerga, eds., *Proc. SPIE* **2280**, pp. 257–271, 1994.

24. K. A. Flanagan, D. Dewey, and B. Bordzol, "Calibration and characterization of HETG grating elements at the MIT x-ray grating evaluation facility," in *EUV, X-Ray, and Gamma-Ray Instrumentation for Astronomy VI*, O. H. Siegmund and J. V. Vallerga, eds., *Proc. SPIE* **2518**, pp. 438–456, 1995.

25. T. H. Markert, D. Dewey, J. E. Davis, K. A. Flanagan, D. E. Graessle, J. M. Bauer, and C. S. Nelson, "Modeling the diffraction efficiencies of the AXAF High-Energy Transmission Grating," in *EUV, X-Ray, and Gamma-Ray Instrumentation for Astronomy VI*, O. H. Siegmund and J. V. Vallerga, eds., *Proc. SPIE* **2518**, pp. 424–437, 1995.

26. K. A. Flanagan, T. T. Fang, C. Baluta, J. E. Davis, D. Dewey, T. H. Markert, D. E. Graessle, J. Drake, J. J. Fitch, J. Z. Juda, J. Woo, S. Kraft, P. Bulicke, R. Fliegauf, S. F, G. Ulm, and J. M. Bauer, "Modeling the diffraction efficiencies of the AXAF High-Energy Transmission Grating: II," in *EUV, X-Ray, and Gamma-Ray Instrumentation for Astronomy VII*, O. H. Siegmund and M. A. Gummin, eds., *Proc. SPIE* **2808**, pp. 650–676, 1996.
27. R. P. Kraft, J. H. Chappell, A. T. Kenter, K. Kobayashi, G. R. Meehan, S. S. Murray, M. V. Zombeck, G. W. Fraser, J. F. Pearson, J. E. Lees, A. N. Brunton, M. Barbera, A. Collura, and S. Serio, "Absolute quantum efficiency calibration of the AXAF High-Resolution Camera," in *EUV, X-Ray, and Gamma-Ray Instrumentation for Astronomy VII*, O. H. Siegmund and M. A. Gummin, eds., *Proc. SPIE* **2808**, pp. 194–209, 1996.
28. A. T. Kenter, J. H. Chappell, K. Kobayashi, R. P. Kraft, G. R. Meehan, S. S. Murray, M. V. Zombeck, G. W. Fraser, J. F. Pearson, J. E. Lees, A. N. Brunton, M. Barbera, A. Collura, and S. Serio, "Performance and calibration of the AXAF High-Resolution Camera I: Imaging read-out," in *EUV, X-Ray, and Gamma-Ray Instrumentation for Astronomy VIII*, O. H. Siegmund and M. A. Gummin, eds., *Proc. SPIE* **3114**, pp. 26–52, 1997.
29. R. P. Kraft, J. H. Chappell, A. T. Kenter, K. Kobayashi, G. R. Meehan, S. S. Murray, M. V. Zombeck, G. W. Fraser, J. F. Pearson, J. E. Lees, A. N. Brunton, M. Barbera, A. Collura, and S. Serio, "Performance and calibration of the AXAF High-Resolution Camera II: Spectroscopic detector," in *EUV, X-Ray, and Gamma-Ray Instrumentation for Astronomy VIII*, O. H. Siegmund and M. A. Gummin, eds., *Proc. SPIE* **3114**, pp. 53–73, 1997.
30. G. R. Meehan, S. S. Murray, M. V. Zombeck, R. P. Kraft, K. Kobayashi, J. H. Chappell, A. T. Kenter, M. Barbera, A. Collura, and S. Serio, "Calibration of the uv/ion shields for the AXAF High-Resolution Camera," in *EUV, X-Ray, and Gamma-Ray Instrumentation for Astronomy VIII*, O. H. Siegmund and M. A. Gummin, eds., *Proc. SPIE* **3114**, pp. 74–100, 1997.
31. G. R. Meehan, A. T. Kenter, R. P. Kraft, S. S. Murray, M. V. Zombeck, K. Kobayashi, J. H. Chappell, M. Barbera, and A. Collura, "Measurement of the transmission of the uv/ion shields for the AXAF High-Resolution Camera," in *EUV, X-Ray, and Gamma-Ray Instrumentation for Astronomy VII*, O. H. Siegmund and M. A. Gummin, eds., *Proc. SPIE* **2808**, 1996.
32. M. Bautz, S. Kissel, G. Prigozhin, S. Jones, T. Isobe, H. Manning, M. Pivovaroff, G. Ricker, and J. Woo, "X-ray CCD calibration for the AXAF CCD Imaging Spectrometer," in *EUV, X-Ray, and Gamma-Ray Instrumentation for Astronomy VII*, O. H. Siegmund and M. A. Gummin, eds., *Proc. SPIE* **2808**, pp. 170–181, 1996.
33. H. L. Manning, S. E. Jones, S. E. Kissel, M. W. Bautz, and G. Ricker, "Quantum efficiency calibration of AXAF CCDs from 2 to 10 keV," in *EUV, X-Ray, and Gamma-Ray Instrumentation for Astronomy VII*, O. H. Siegmund and M. A. Gummin, eds., *Proc. SPIE* **2808**, pp. 23–33, 1996.
34. G. Y. Prigozhin, M. W. Bautz, and K. Gendreauand G. R. Ricker, "Calibration of x-ray CCDs with an erect-field grating spectrometer in the 0.2-to-1.5-keV band," in *EUV, X-Ray, and Gamma-Ray Instrumentation for Astronomy VII*, O. H. Siegmund and M. A. Gummin, eds., *Proc. SPIE* **2808**, pp. 260–270, 1996.
35. L. K. Townsley, P. S. Broos, and J. F. Mackay, "Transmission maps of the ACIS uv/optical blocking filter flight units," *Bull. Am. Astron. Soc.* **188**, p. 5501, 1996.
36. G. Chartas, G. Garmire, J. Nousek, D. Graessle, and L. Furenlid, "Measuring the x-ray transmission function of the ACIS uv/optical blocking filters at the National Synchrotron Light Source," *Bull. Am. Astron. Soc.* **188**, p. 5503, 1996.
37. P. Zhao, R. A. Austin, R. J. Edgar, R. F. Elsner, T. J. Gaetz, D. Jerius, J. J. Kolodziejczak, W. C. McDermott, S. L. O'Dell, M. E. Sulkanen, D. A. Schwartz, D. A. Swartz, A. F. Tennant, L. P. Van Speybroeck, B. J. Wargelin, M. C. Weisskopf, and G. Zirnstein, "AXAF mirror effective-area calibration using the C-continuum source and solid-state detectors," in *X-Ray Optics, Instruments, and Missions*, R. B. Hoover and A. B. Walker, eds., *Proc. SPIE* **3444**, these proceedings, 1998.
38. J. Nousek, L. Townsley, G. Chartas, D. Burrows, E. Moskalenko, R. Sambruna, J. Pesce, C. Grant, K. Nishikida, L. Cawley, P. Broos, T. S. Koch, A. Garmire, G. Garmire, M. Bautz, S. Jones, B. LaMarr, and G. Ricker, "Joint AXAF High-Resolution Mirror Assembly and AXAF CCD Imaging Spectrometer calibration at the MSFC X-Ray Calibraton Facility," in *X-Ray Optics, Instruments, and Missions*, R. B. Hoover and A. B. Walker, eds., *Proc. SPIE* **3444**, these proceedings, 1998.
39. G. Chartas, G. Garmire, J. Nousek, S. Koch, S. Kissel, S. Prigozhin, and M. Bautz, "Optimizing the ACIS effective area and energy resolution," in *X-Ray Optics, Instruments, and Missions*, R. B. Hoover and A. B. Walker, eds., *Proc. SPIE* **3444**, these proceedings, 1998.

40. D. Dewey, J. J. Drake, R. J. Edgar, K. Michaud, and P. Ratzlaff, "AXAF grating-efficiency measurements with calibrated, non-imaging detectors," in *X-Ray Optics, Instruments, and Missions*, R. B. Hoover and A. B. Walker, eds., *Proc. SPIE* **3444**, these proceedings, 1998.
41. N. S. Schulz, D. Dewey, and H. L. Marshall, "Absolute effective areas of the HETGS," in *X-Ray Optics, Instruments, and Missions*, R. B. Hoover and A. B. Walker, eds., *Proc. SPIE* **3444**, these proceedings, 1998.
42. E. M. Kellogg, L. Cohen, R. J. Edgar, I. N. Evans, M. Freeman, T. Gaetz, D. Jerius, W. C. McDermott, P. McKinnon, S. S. Murray, W. Podgorski, D. A. Schwartz, L. P. Van Speybroeck, B. Wargelin, M. V. Zombeck, M. C. Weisskopf, R. F. Elsner, S. L. O'Dell, B. D. Ramsey, A. F. Tennant, J. J. Kolodziejczak, G. Garmire, J. Nousek, S. Kraft, F. Scholze, R. Thornagel, G. Ulm, K. Flanagan, D. Dewey, M. Bautz, S. Texter, J. Arenberg, and R. Carlson, "Absolute calibration of the AXAF telescope effective area," in *Grazing Incidence and Multilayer X-Ray Optical Systems*, R. B. Hoover and A. B. Walker, eds., *Proc. SPIE* **3113**, pp. 515–525, 1997.
43. J. J. Kolodziejczak, R. A. Austin, R. F. Elsner, S. L. O'Dell, M. E. Sulkanen, D. A. Swartz, A. F. Tennant, M. C. Weisskopf, G. Zirnstein, and W. C. McDermott, "Uses of continuum radiation in the AXAF calibration," in *Grazing Incidence and Multilayer X-Ray Optical Systems*, R. B. Hoover and A. B. Walker, eds., *Proc. SPIE* **3113**, pp. 65–76, 1997.
44. A. C. Brinkman, C. J. T. Gunsing, J. S. Kaastra, H. Bräuninger, G. Hartner, P. Predehl, J. J. Drake, J. Z. Juda, M. Juda, D. Dewey, K. A. Flanagan, and H. L. Marshall, "Preliminary test results on spectral resolution of the Low-Energy Transmission Grating Spectrometer on board AXAF," in *Grazing Incidence and Multilayer X-Ray Optical Systems*, R. B. Hoover and A. B. Walker, eds., *Proc. SPIE* **3113**, pp. 181–192, 1997.
45. P. Predehl, H. Bräuninger, A. C. Brinkman, D. Dewey, J. J. Drake, K. A. Flanagan, T. Gunsing, G. D. Hartner, J. Z. Juda, M. Juda, J. Kaastra, H. L. Marshall, and D. Swartz, "X-ray calibration of the AXAF Low-Energy Transmission Grating Spectrometer: Effective area," in *Grazing Incidence and Multilayer X-Ray Optical Systems*, R. B. Hoover and A. B. Walker, eds., *Proc. SPIE* **3113**, pp. 172–180, 1997.
46. H. L. Marshall, D. Dewey, K. A. Flanagan, C. Baluta, C. R. Canizares, D. S. Davis, J. E. Davis, T. T. Fang, D. P. Huenemoerder, J. H. Kastner, N. S. Schulz, M. W. Wise, J. J. Drake, J. Z. Juda, M. Juda, A. C. Brinkman, C. J. T. Gunsing, J. S. Kaastra, G. Hartner, and P. Predehl, "Towards the calibration of the HETGS line response function," in *Grazing Incidence and Multilayer X-Ray Optical Systems*, R. B. Hoover and A. B. Walker, eds., *Proc. SPIE* **3113**, pp. 160–171, 1997.
47. D. Dewey, K. A. Flanagan, H. L. Marshall, C. Baluta, C. R. Canizares, D. S. Davis, J. E. Davis, T. T. Fang, D. P. Huenemoerder, J. H. Kastner, N. S. Schulz, M. W. Wise, J. J. Drake, J. Z. Juda, M. Juda, A. C. Brinkman, C. J. T. Gunsing, J. S. Kaastra, G. Hartner, and P. Predehl, "Towards the calibration of the HETGS effective area," in *Grazing Incidence and Multilayer X-Ray Optical Systems*, R. B. Hoover and A. B. Walker, eds., *Proc. SPIE* **3113**, pp. 144–159, 1997.
48. L. Nevot and P. Croce, "Caractérisation des surfaces par réflexion rasant de rayons x: application á l'étude du polissage de quelques verres silicates," *Rev. Phys. Appl.* **15**, pp. 761–779, 1980.
49. L. Nevot, B. Pardo, and J. Corno, "Characterization of x–uv multilayers by grazing-incidence x-ray reflectometry," *Rev. Phys. Appl.* **23**, pp. 1675–1686, 1980.
50. P. Beckmann and A. Spizzichino, *The Scattering of Electromagnetic Waves from Rough Surfaces*, Pergamon Press, New York, New York, 1963.
51. D. E. Graessle, R. L. Blake, A. J. Burek, S. E. Dyson, J. J. Fitch, D. A. Schwartz, and R. Soufli, "Modeling of synchrotron reflectance measurements of AXAF iridium-coated witness mirrors over 2–12 keV," in *X-Ray Optics, Instruments, and Missions*, R. B. Hoover and A. B. Walker, eds., *Proc. SPIE* **3444**, these proceedings, 1998.
52. R. F. Elsner, S. L. O'Dell, and M. C. Weisskopf, "Molecular contamination and the calibration of AXAF," in *Multilayer and grazing incidence X-ray/EUV optics for astronomy and projection lithography*, R. B. Hoover and A. B. Walker, eds., *Proc. SPIE* **1742**, pp. 6–12, 1993.
53. D. E. Graessle, T. H. Burbine, J. J. Fitch, W. A. Podgorski, J. Z. Juda, R. F. Elsner, S. L. O'Dell, and J. M. Reynolds, "Molecular contamination study of iridium-coated x-ray mirrors," in *Advances in Multilayer and Grazing Incidence X-Ray/EUV/FUV Optics*, R. B. Hoover and A. B. Walker, eds., *Proc. SPIE* **2279**, pp. 12–26, 1994.
54. P. S. Boos, L. K. Townsley, and J. Nousek, "Discarding piled-up events in ACIS," in *X-Ray Optics, Instruments, and Missions*, R. B. Hoover and A. B. Walker, eds., *Proc. SPIE* **3444**, these proceedings, 1998.